

International Journal of Modern Physics A
© World Scientific Publishing Company

Quantum Vacuum Self-Propulsion and Torque

Kimball A. Milton

*H.L. Dodge Department of Physics and Astronomy,
Norman, OK 73019 USA
kmilton@ou.edu*

Nima Pourtolami

*National Bank of Canada
Montreal, Quebec H3B 4S9 Canada
nima.pourtolami@gmail.com*

Gerard Kennedy

*School of Mathematical Sciences, University of Southampton
Southampton SO17 1BJ UK
g.kennedy@soton.ac.uk*

Received Day Month Year

Revised Day Month Year

This article summarizes our recent efforts to understand spontaneous quantum vacuum forces and torques, which require that a stationary object be out of thermal equilibrium with the blackbody background radiation. We proceed by a systematic expansion in powers of the electric susceptibility. In first order, no spontaneous force can arise, although a torque can appear, but only if the body is composed of nonreciprocal material. In second order, both forces and torques can appear, with ordinary materials, but only if the body is inhomogeneous. In higher orders, this last requirement may be removed. We give a number of examples of bodies displaying second-order spontaneous forces and torques, some of which might be amenable to observation.

Keywords: Spontaneous vacuum force; spontaneous vacuum torque; nonequilibrium phenomena.

PACS numbers: 42.50.Lc, 05.70.Ln, 68.35.Af

1. Introduction

Growing out of our explorations of quantum (Casimir) friction,¹⁻³ we are studying the forces and torques arising on bodies in vacuum out of thermal equilibrium. A torque can arise in first order in susceptibility for a body that is nonreciprocal. This is described in more detail in Refs. 4, 5. For a reciprocal body, spontaneous torques and forces require not only nonequilibrium but inhomogeneity of the body. Such effects emerge in second order. More detail on spontaneous forces and torques can be found in Refs. 6, 7. See these papers for fuller references to the literature.

2 Milton, Pourtolami, Kennedy

We use natural units, $\hbar = c = \epsilon_0 = \mu_0 = k_B = 1$.

2. Quantum Vacuum Torque in Nonreciprocal Media

This phenomenon was first discussed in Ref. 8, and then subsequently in our paper, Ref. 4. We summarize the latter here.

Classically, the torque on a stationary dielectric body with polarization vector \mathbf{P} is given by⁹

$$\boldsymbol{\tau} = \int (d\mathbf{r}) \frac{d\omega}{2\pi} \frac{d\nu}{2\pi} e^{-i(\omega+\nu)t} [\mathbf{P}(\mathbf{r}; \omega) \times \mathbf{E}(\mathbf{r}; \nu) + P_i(\mathbf{r}; \omega) (\mathbf{r} \times \nabla) E_i(\mathbf{r}; \nu)]. \quad (1)$$

The first term here is called the *internal* torque and the second the *external* torque, because the latter is reflective of the force on the body. We expand this out to first order in generalized susceptibilities, using

$$\mathbf{E}^{(1)}(\mathbf{r}; \omega) = \int (d\mathbf{r}') \boldsymbol{\Gamma}(\mathbf{r} - \mathbf{r}'; \omega) \cdot \mathbf{P}(\mathbf{r}'; \omega), \quad \mathbf{P}^{(1)}(\mathbf{r}; \omega) = \boldsymbol{\chi}(\mathbf{r}; \omega) \cdot \mathbf{E}(\mathbf{r}; \omega), \quad (2)$$

in terms of the (local) electric susceptibility $\boldsymbol{\chi}$ and the (vacuum) electromagnetic Green's dyadic $\boldsymbol{\Gamma}$. We evaluate the two contributions (PP and EE) to the quantum vacuum torque by use of the fluctuation-dissipation theorem (FDT):

$$\langle \mathbf{P}_i(\mathbf{r}; \omega) \mathbf{P}_j(\mathbf{r}'; \nu) \rangle = 2\pi \delta(\omega + \nu) \delta(\mathbf{r} - \mathbf{r}') \boldsymbol{\chi}_{ij}^A(\mathbf{r}; \omega) \coth \frac{\beta' \omega}{2}, \quad (3a)$$

$$\langle \mathbf{E}_i(\mathbf{r}; \omega) \mathbf{E}_j(\mathbf{r}'; \nu) \rangle = 2\pi \delta(\omega + \nu) \Im \boldsymbol{\Gamma}_{ij}(\mathbf{r} - \mathbf{r}'; \omega) \coth \frac{\beta \omega}{2}, \quad (3b)$$

in terms of the inverse temperatures of the vacuum background, $\beta = 1/T$, and of the body, $\beta' = 1/T'$.

Here, $\boldsymbol{\Gamma}$ is taken to be the usual vacuum retarded Green's dyadic, which at coincident points is (rotationally averaged)

$$\boldsymbol{\Gamma}(\mathbf{r} - \mathbf{r}'; \omega) \rightarrow \mathbf{1} \left(\frac{\omega^2}{6\pi R} + i \frac{\omega^3}{6\pi} + O(R) \right), \quad R = |\mathbf{r} - \mathbf{r}'| \rightarrow 0, \quad (4)$$

while $\boldsymbol{\chi}^A$ is the anti-Hermitian part of the susceptibility:

$$\boldsymbol{\chi}^A = \frac{1}{2i} (\boldsymbol{\chi} - \boldsymbol{\chi}^\dagger), \quad \Im \boldsymbol{\chi}_{ij}^A(\omega) = -\frac{1}{2} \Re [\chi_{ij}(\omega) - \chi_{ji}(\omega)], \quad (5)$$

which displays the antisymmetric part of $\boldsymbol{\chi}^A$, which is even in ω . The real part of $\boldsymbol{\chi}^A$ is symmetric in indices and odd in ω . Only the former contributes to the torque.

Using this, we readily calculate the torque on a nonreciprocal body in vacuum, due to PP and EE fluctuations:

$$\tau_i = - \int_{-\infty}^{\infty} \frac{d\omega}{2\pi} \frac{\omega^3}{6\pi} \left[\coth \frac{\beta' \omega}{2} - \coth \frac{\beta \omega}{2} \right] \epsilon_{ijk} \Re \alpha_{jk}(\omega), \quad (6)$$

where the mean polarizability of the body is given by $\alpha_{jk}(\omega) = \int (d\mathbf{r}) \chi_{jk}(\mathbf{r}; \omega)$. This result exactly agrees with that of Strehka et al.⁸ However, there is no quantum vacuum force in this static situation. To create a nonreciprocal medium typically requires an external magnetic field, so this is not exactly a pure vacuum

phenomenon. If the nonreciprocity is generated by a magnetic field of 1 T, the corresponding torque for a gold nanoball of radius 100 nm is $\sim 10^{-24}$ Nm for $T' = 600$ K, $T = 300$ K.

3. Self-Propulsive Force

The Lorentz force on a dielectric body is,⁹ where we have omitted a term which vanishes when the FDT is used,

$$\mathbf{F} = - \int (d\mathbf{r}) \int \frac{d\omega}{2\pi} \frac{d\nu}{2\pi} e^{-i(\omega+\nu)t} \frac{\omega}{\nu} P_i(\mathbf{r}; \omega) \cdot (\nabla) \cdot E_i(\mathbf{r}; \nu). \quad (7)$$

Now we expand the fields out to second order (4th order in generalized susceptibilities, χ and Γ , after use of the FDT):

$$\mathbf{E}^{(2)}(\mathbf{r}; \nu) = \int (d\mathbf{r}') \Gamma(\mathbf{r} - \mathbf{r}'; \nu) \cdot \chi(\mathbf{r}'; \nu) \cdot \mathbf{E}(\mathbf{r}'; \nu), \quad (8a)$$

$$\mathbf{E}^{(3)}(\mathbf{r}; \nu) = \int (d\mathbf{r}') (d\mathbf{r}'') \Gamma(\mathbf{r} - \mathbf{r}'; \nu) \cdot \chi(\mathbf{r}'; \nu) \cdot \Gamma(\mathbf{r}' - \mathbf{r}''; \nu) \cdot \mathbf{P}(\mathbf{r}''; \nu), \quad (8b)$$

$$\mathbf{P}^{(2)}(\mathbf{r}; \omega) = \int (d\mathbf{r}') \chi(\mathbf{r}; \omega) \cdot \Gamma(\mathbf{r} - \mathbf{r}'; \omega) \cdot \mathbf{P}(\mathbf{r}'; \omega), \quad (8c)$$

$$\mathbf{P}^{(3)}(\mathbf{r}; \omega) = \int (d\mathbf{r}') \chi(\mathbf{r}; \omega) \cdot \Gamma(\mathbf{r} - \mathbf{r}'; \omega) \cdot \chi(\mathbf{r}'; \omega) \cdot \mathbf{E}(\mathbf{r}'; \omega). \quad (8d)$$

Using the symmetries of the integrand we find the following general expression for the force on a body composed of isotropic material:

$$\begin{aligned} \mathbf{F} = \int (d\mathbf{r}) (d\mathbf{r}') \int_{-\infty}^{\infty} \frac{d\omega}{2\pi} X(\mathbf{r}, \mathbf{r}'; \omega) \Im \Gamma_{ji}(\mathbf{r}' - \mathbf{r}; \omega) \\ \times \nabla \Im \Gamma_{ij}(\mathbf{r} - \mathbf{r}'; \omega) \left[\coth \frac{\beta\omega}{2} - \coth \frac{\beta'\omega}{2} \right], \end{aligned} \quad (9)$$

where the second-order susceptibility product is

$$X(\mathbf{r}, \mathbf{r}'; \omega) = \Im \chi(\mathbf{r}; \omega) \Re \chi(\mathbf{r}'; \omega) - \Re \chi(\mathbf{r}; \omega) \Im \chi(\mathbf{r}'; \omega). \quad (10)$$

Obviously, if the body is homogeneous, so the susceptibility is independent of position, then X vanishes, and there is no force on the body.

Consider a body composed of two parts, each of which is separately made of homogeneous material. In such a case, the force in the z direction reduces to

$$F_z = 8 \int_0^{\infty} \frac{d\omega}{2\pi} X_{AB}(\omega) I_{AB}(\omega) \left[\frac{1}{e^{\beta\omega} - 1} - \frac{1}{e^{\beta'\omega} - 1} \right], \quad (11)$$

where the geometric integral is

$$I_{AB}(\omega) = \int_A (d\mathbf{r}) \int_B (d\mathbf{r}') \frac{1}{2} \nabla_z [\Im \Gamma_{ji}(\mathbf{r}' - \mathbf{r}; \omega) \Im \Gamma_{ij}(\mathbf{r} - \mathbf{r}'; \omega)], \quad (12)$$

and the susceptibility product becomes

$$X_{AB}(\omega) = \Im \chi_A(\omega) \Re \chi_B(\omega) - \Re \chi_A(\omega) \Im \chi_B(\omega). \quad (13)$$

4 Milton, Pourtolami, Kennedy

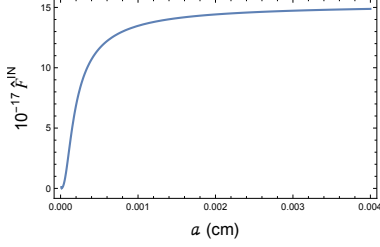


Fig. 1. Force (\hat{F}) on inhomogeneous needle for $a = b$ when $T = 300$ K and $T' = 600$ K. Note the saturation for large a ; only the immediate region near the A - B interface contributes. The saturated force (F) is about $0.03\chi_A$ N.

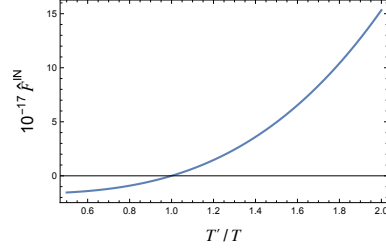


Fig. 2. Dependence of force (\hat{F}) on T' for $T = 300$ K. $a = b = 1$ cm.

From the form of the vacuum electromagnetic Green's dyadic,

$$\mathbf{\Gamma}'(\mathbf{r} - \mathbf{r}'; \omega) = (\nabla\nabla - \mathbf{1}\nabla^2) \frac{e^{i\omega R}}{4\pi R}, \quad \mathbf{\Gamma}' = \mathbf{\Gamma} + \mathbf{1}, \quad (14)$$

we find for the gradient of the product of the imaginary parts of $\mathbf{\Gamma}$

$$\frac{1}{2} \nabla [\Im \Gamma_{ji}(-\mathbf{R}; \omega) \Im \Gamma_{ij}(\mathbf{R}; \omega)] = \frac{1}{(4\pi)^2} \frac{\mathbf{R}}{R^8} \phi(v), \quad \mathbf{R} = \mathbf{r} - \mathbf{r}', \quad v = \omega R, \quad (15)$$

where

$$\phi(v) = -9 - 2v^2 - v^4 + (9 - 16v^2 + 3v^4) \cos 2v + v(18 - 8v^2 + v^4) \sin 2v. \quad (16)$$

The limiting behaviors are

$$\phi(v) \sim -\frac{4}{9}v^8 + \frac{28}{225}v^{10} + \dots, \quad v \ll 1, \quad \phi(v) \sim -v^4 + v^5 \sin 2v + 3v^4 \cos 2v + \dots, \quad v \gg 1. \quad (17)$$

Example 1: Thin inhomogeneous needle. The susceptibility of a thin needle of cross section S with parts A and B of length a and b made of different materials is

$$\chi(\mathbf{r}; \omega) = S [\delta(x)\delta(y)\theta(z)\theta(a-z)\chi_A(\omega) + \delta(x)\delta(y)\theta(-z)\theta(b+z)\chi_B(\omega)]. \quad (18)$$

For definiteness, chose χ_A to be a real constant (frequencies small compared to binding energies), while B is taken to be a Drude-type metal

$$\chi_B(\omega) = -\frac{\omega_p^2}{\omega^2 + i\omega\nu}. \quad (19)$$

For gold, with the vacuum at $T = 300$ K, and the cross-sectional radius of the needle being 1 mm, the force is about ($a_0 = 1$ cm, $\beta_0 = 40$ (eV) $^{-1}$)

$$F = -\frac{S^2 \omega_p^2 \nu \chi_A \beta_0^2}{120\pi^3 a_0^5} \hat{F} = -2\chi_A \times 10^{-20} \hat{F} \text{ N}, \quad (20)$$

where \hat{F} for gold is shown in Figs. 1 and 2. Since $\hat{F} \sim 10^{18}$, this seems very large.

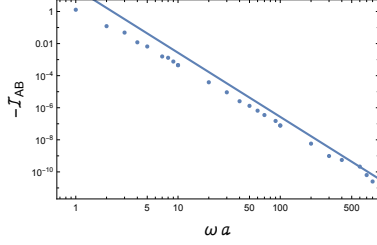


Fig. 3. Numerical integration of I_{AB} , apart from the prefactor $\omega^8 a^5 t / (8\pi)$, is shown by the dots. The solid line shows that the asymptotic value of $\phi(v) \sim -v^4$ leads to the power-law behavior $\mathcal{N}/(\omega a)^4$ with $\mathcal{N} \approx -27$.

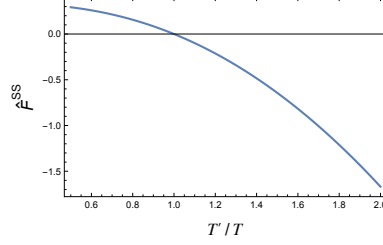


Fig. 4. Dimensionless force \hat{F} as a function of the temperature of the spherical shell relative to the room-temperature background.

However, this is probably overly optimistic. For the validity of our weak-susceptibility model, we need the needle to be much thinner than 1 mm. The appropriate scale would seem to be the skin depth, which is⁹

$$\delta = (\omega\sigma/2)^{-1/2} = (\omega^2 \Im\chi/2)^{-1/2} = \sqrt{\frac{2(\omega^2 + \nu^2)}{\omega\omega_p^2\nu}} \sim 50 \text{ nm}, \quad (21)$$

which reduces this force substantially (by a factor of 10^{-17}).

Example 2: Thin spherical shell. Consider next a thin spherical shell of radius a and thickness t . Suppose the upper and lower hemispheres have different uniform susceptibilities

$$\chi(\mathbf{r}; \omega) = \begin{cases} 0 < \theta < \frac{\pi}{2} : \chi_A(\omega), \\ \frac{\pi}{2} < \theta < \pi : \chi_B(\omega). \end{cases} \quad (22)$$

In this case the geometric integral I_{AB} is shown in Fig. 3.

The force on the thin spherical shell is

$$F = -\frac{\omega_p^2 t^2 a}{16\pi^2} \chi_A \nu^3 \mathcal{N} \hat{F} \approx 1 \times 10^{-12} \chi_A \hat{F} \text{ N} \quad (23)$$

for gold, with the thickness of the shell being $t = 2/\omega_p$ (minimum value of skin depth), and the radius of the shell being $a = 1 \text{ cm}$. The dimensionless force \hat{F} is shown in Fig. 4.

Example 3. Janus ball. We now consider a ball, of radius a , each half-ball, A and B , being composed of a different homogeneous material. Then the geometric integral for such a ball is shown in Fig. 5.

The spontaneous force on a small Janus ball of radius $1 \mu\text{m}$, with A inert and B gold, is

$$F^{\text{JB}} = \frac{1}{27\pi} \chi_A \omega_p^2 (\nu a)^7 \hat{F} \approx 4 \times 10^{-18} \chi_A \hat{F} \text{ N}. \quad (24)$$

6 Milton, Pourtolami, Kennedy

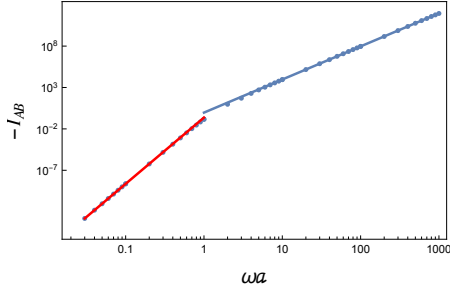


Fig. 5. The geometric integral for a Janus ball, scaled by $8\pi a$, is given by the dots, as a function of ωa . The straight lines show the large $\sim (\omega a)^4$ and small $\sim (\omega a)^8$ behaviors.

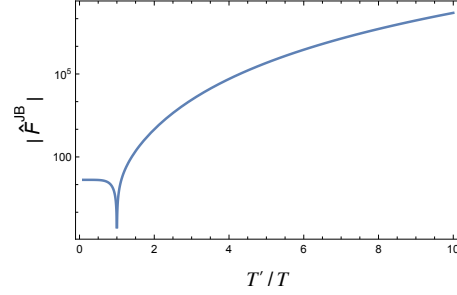


Fig. 6. Semilog plot of the magnitude of the force on a Janus ball as a function of the temperature of the ball, relative to that of the room-temperature background. The force is negative if the ball is hotter than the blackbody background.

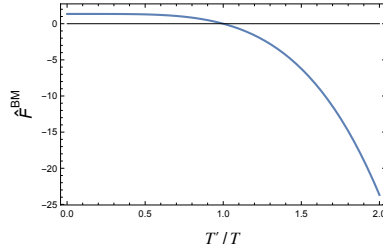


Fig. 7. Dimensionless force on a blackbody-metal plate.

The dimensionless force is shown in Fig. 6 for $T = 300$ K. The result may be compared with the nonperturbative numerical results of Ref. 10; the numbers are similar, but the scaling with a is different.

Example 4: Planar structure. We consider a thin planar object, which consists of blackbody material on the upper side, A , and a Drude metal on the lower, B . By a blackbody material we mean one whose surface susceptibility, $\tilde{\chi} = \frac{V}{S}\chi$, V and S being the volume and the surface area of the body, is

$$\tilde{\chi} = \frac{i}{4} \frac{1}{\omega + i\epsilon}, \quad \epsilon \rightarrow +0, \quad (25)$$

since this will yield Stefan's law for the radiated power, $P = S\pi^2(T^4 - T'^4)/60$. If the thicknesses of the two sides are t_A and t_B , the force is

$$F_z = \frac{St_B(t_A + t_B)\omega_p^2\nu^4}{24\pi^2} \hat{F}, \quad (26)$$

where \hat{F} is shown in Fig. 7. For $S = 1$ cm², $t_A = t_B = 10$ nm, and the metal being gold, the prefactor in the force is 4×10^{-13} N, corresponding to an acceleration of ~ 40 m/s². Comparable results were found in Ref. 11. In this case, as in the

other examples, the force is always towards the metal side of the object (in our convention, negative).

3.1. Friction and thermalization lead to terminal velocity

Once the body starts to move due to the nonequilibrium quantum force, it will experience quantum friction, nonrelativistically given by the Einstein-Hopf formula,

$$F_f = -\frac{v\beta}{12\pi^2} \int_0^\infty d\omega \omega^5 \Im \alpha(\omega) \frac{1}{\sinh^2 \beta\omega/2}, \quad (27)$$

and, therefore, it will reach a terminal velocity:

$$v(t) = v_T \left(1 - e^{-t/t_0}\right). \quad (28)$$

For example, a needle having a 1 cm half-length and 10 nm radius, would have a terminal velocity of order 5 m/s. But the time scale, $t_0 \sim 15$ yrs, is very long.

More important is thermal cooling. Unless there is some mechanism supplied to maintain the temperature difference, the body will eventually cool to the temperature of the environment. From Newton's law, the terminal velocity is

$$v_T = \frac{1}{m} \int_0^\infty dt F(T'(t), T). \quad (29)$$

Here, the cooling rate is given by

$$\frac{dQ}{dt} = C_V(T') \frac{dT'}{dt} = P(T', T), \quad (30)$$

where $C_V(T')$ is the specific heat of the body at temperature T' . For a slowly moving body the power radiated is²

$$P(T', T) = \frac{1}{3\pi^2} \int_0^\infty d\omega \omega^4 \Im \text{tr } \alpha(\omega) \left[\frac{1}{e^{\beta\omega} - 1} - \frac{1}{e^{\beta'\omega} - 1} \right]. \quad (31)$$

In terms of $u = T'/T$, the time taken for the body to cool from temperature T'_0 to temperature T'_1 , $T'_0 > T'_1 > T$, is (for temperatures well above the Debye temperature)

$$t_1 = \int_{T'_0}^{T'_1} dT' \frac{C_V(T')}{P(T', T)}, \quad \text{or} \quad \frac{t_1}{t_c} = \int_{u_0}^{u_1} du \frac{1}{p(u; T)}, \quad (32)$$

where the dimensionless power radiated is modeled by⁴

$$p(u; T) = \int_0^\infty dx \frac{x^3}{x^2 + 1} \left(\frac{1}{e^{\beta\nu x} - 1} - \frac{1}{e^{\beta\nu x/u} - 1} \right). \quad (33)$$

Therefore, the terminal velocity is

$$v_T = \frac{t_c}{m} \int_{u_0}^1 du \frac{F(u; T)}{p(u; T)}. \quad (34)$$

8 *Milton, Pourtolami, Kennedy*

The time scale for a weak susceptibility model of the metal portion of an object is

$$t_c = \frac{3\pi^2 n T}{\nu^3 \omega_p^2} \sim 10^{-4} \text{ s}, \quad n = \text{number density}, \quad (35)$$

For a Janus ball, of radius 100 nm, half made of gold and half dielectric, with an initial temperature twice that of the background, the terminal velocity is only about 0.1 nm/s. For a spherical shell model with radius 1 cm and skin-depth thickness, v_T would be about the same. So, observation might prove challenging.

4. Spontaneous Torque on an Inhomogeneous Chiral Body

In Sec. 2, we calculated the torque in first order, which required the body be composed of nonreciprocal material, which usually necessitates an external field be applied. In second order, a torque can arise on a reciprocal body, but again only if the body is *inhomogeneous*. It must further be *chiral*, in that its mirror reflection cannot be turned into the original object by translations or rotations.

For a body with isotropic but inhomogeneous susceptibility there is only an external torque, calculated in second order:

$$\begin{aligned} \tau_i = & \int \frac{d\omega}{2\pi} \left(\coth \frac{\beta\omega}{2} - \coth \frac{\beta'\omega}{2} \right) \epsilon_{ijk} \int (d\mathbf{r})(d\mathbf{r}') X(\mathbf{r}, \mathbf{r}'; \omega) \\ & \times \Im \Gamma_{lm}(\mathbf{r} - \mathbf{r}'; \omega) r_j \nabla_k \Im \Gamma_{ml}(\mathbf{r}' - \mathbf{r}; \omega). \end{aligned} \quad (36)$$

Again the susceptibility product X [Eq. (10)] vanishes if the body is homogeneous. If the body consists of two homogeneous parts, A and B , X is replaced by X_{AB} defined in Eq. (13). Using Eq. (15), we find the torque in this situation is

$$\boldsymbol{\tau} = \frac{1}{2\pi^2} \int_0^\infty \frac{d\omega}{2\pi} X_{AB}(\omega) \left(\frac{1}{e^{\beta\omega} - 1} - \frac{1}{e^{\beta'\omega} - 1} \right) \mathbf{J}_{AB}(\omega), \quad (37a)$$

in terms of the geometric factor

$$\mathbf{J}_{AB}(\omega) = - \int_A (d\mathbf{r}) \int_B (d\mathbf{r}') \frac{\mathbf{r} \times \mathbf{r}'}{|\mathbf{r} - \mathbf{r}'|^8} \phi(\omega|\mathbf{r} - \mathbf{r}'|). \quad (37b)$$

That the integral is convergent is evident from the behavior of ϕ given in Eq. (17).

Examples: Dual Allen wrench and dual flags. A simple example of an inhomogeneous chiral object is shown in Fig. 8, which illustrates what we might refer to as a dual Allen wrench. This object will experience a quantum vacuum torque, but not a net force, because it is reflection invariant in the origin, $\mathbf{r} \rightarrow -\mathbf{r}$. The geometric factor for this object, which points in the direction perpendicular to the plane of the object, is

$$J_{AB}(\omega) = 2S_A S_B \omega^8 \int_{-a}^a dy \int_0^b dx xy \frac{\phi(v)}{v^8}, \quad v = \omega \sqrt{x^2 + (a+y)^2}. \quad (38)$$

J_{AB} , apart from a prefactor of $2\omega^4 S_A S_B$, where S_i is the cross-sectional area of the i th wire, is shown in the Fig. 10 in terms of $\tilde{a} = \omega a$.

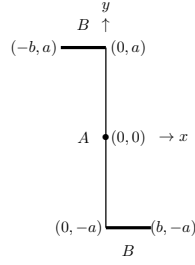


Fig. 8. An inhomogeneous wire of small cross section bent in the shape of a dual Allen wrench. The end pieces (“tags”) B are taken to be dispersionless dielectric, while the central piece A is a Drude-type metal. The Cartesian coordinates of the various junctions are shown, as is the center of mass.

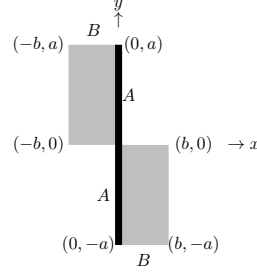


Fig. 9. Planar inhomogeneous object, obtained by replacing the tags by flags.

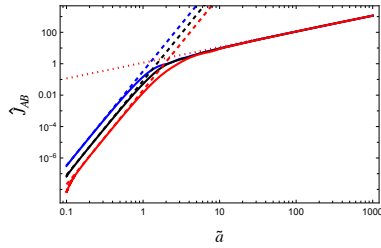


Fig. 10. Scaled geometric factor as a function of the length of the central wire, $\tilde{a} = a\omega$, for different values of $b = a/2$, a , or $2a$ from bottom to top. These are compared with the asymptotes for large- (dotted) and small- (dashed) arguments.

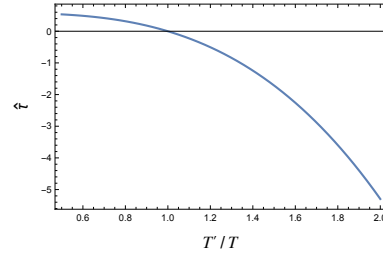
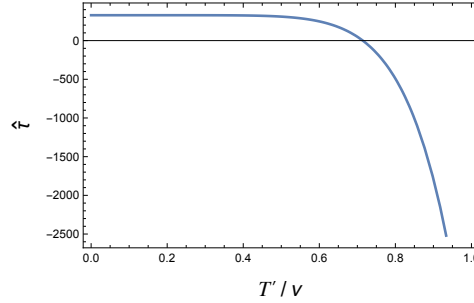


Fig. 11. Torque, apart from the prefactor, on a large Allen wrench, as a function of its temperature relative to the room-temperature background.

The large \tilde{a} behavior is easily understood: the interactions between the parts are local, so increasing b beyond a certain point does not increase the torque. The local forces on A due to the tags B are also saturated as a increases, but the lever arm increases linearly. The asymptotic value of J_{AB} , apart from the same prefactor, is $\hat{J}_{AB} \sim 11\pi\omega a/30$ for $\omega a \gg 1$. Around room temperature, the transition from large to small occurs at $a, b \sim 10 \mu\text{m}$. The torque on a large Allen wrench is

$$\tau = \frac{11}{60\pi^2} S_A S_B a \nu^4 \omega_p^2 \chi_B \hat{\tau}, \quad \hat{\tau} = \int_0^\infty dx \frac{x^4}{x^2 + 1} \left(\frac{1}{e^{\beta\nu x} - 1} - \frac{1}{e^{\beta'\nu x} - 1} \right). \quad (39)$$

For a gold wire of circular radius 50 nm, and length $a = 1$ cm, the prefactor,

10 *Milton, Pourtolami, Kennedy*Fig. 12. Torque, $\hat{\tau}$, on a small Allen wrench.

τ_0 , is 7×10^{-22} N m. The integral, $\hat{\tau}$, is shown in Fig. 11. Such a torque might well be observable, although the terminal angular velocity due to cooling is small, $\omega_T \sim 10^{-9}$ s $^{-1}$, if the initial temperature $T' = 2T$.

The situation might be much more favorable for a small object. If $\omega a, \omega b \ll 1$, the geometric integral is, of course, much smaller, $\hat{J}_{AB} = 56\omega^6 a^4 b^2 / 675$. Now, the corresponding torque is

$$\tau = \frac{28}{675\pi^3} \chi_B \nu^9 \omega_p^2 S_A S_B a^4 b^2 \hat{\tau}. \quad (40)$$

where $\hat{\tau}$ is shown in Fig. 12. In this case, the terminal angular velocity is much larger, because the moment of inertia of the object is much smaller as well,

$$I = \rho_A S_A \frac{2}{3} a^3 + \rho_B S_B 2b \left(a^2 + \frac{1}{3} b^2 \right). \quad (41)$$

so the resulting terminal angular velocity due to thermal cooling is

$$\omega_T = \frac{t_c \tau_0}{I} \hat{\omega}_T, \quad \hat{\omega}_T = \int_{T'_0/T}^1 du \frac{\hat{\tau}(u; T)}{p(u; T)} \quad (42)$$

where the prefactor $t_c \tau_0 / I \sim 2 \times 10^{-7}$ s $^{-1}$ for a 1 μ m object, and p is given by Eq. (33). Because the dimensionless torque is large, so is $\hat{\omega}_T \sim 20,000$, if the initial temperature of the object is twice that of the room temperature environment, leading to a large terminal angular velocity, $\omega_T \sim 4 \times 10^{-3}$ s $^{-1}$, which should be quite observable.

Further enhancement of the terminal angular velocity, by about a factor of 10^5 for a large (1 cm) object or by about a factor of 10 for a small (1 μ m) object, can be achieved by increasing the size of the tags, so we have a dual flag shown in Fig. 9. Terminal angular velocities for both large and small dual flags would seem to be easily accessible to experimental observation.

5. Conclusions

- In first order in electric susceptibility, a vacuum torque, but no force, can arise for a body made of *nonreciprocal* material.

- In second order, a vacuum force can arise only if the body is *inhomogeneous*, but no exotic material properties are required.
- A vacuum torque can also arise for ordinary chiral bodies in second order, but again only if the body is also *inhomogeneous*. This is in contrast to the findings of Ref. 10.
- We consider several examples of bodies which exhibit possibly observable vacuum forces and torques, although cooling to equilibrium with the vacuum environment may make it challenging to observe the resulting linear and angular terminal velocities, unless the temperature imbalance is maintained. The terminal angular velocity for a dual flag appears measurable.
- For dielectric-metal bodies, the force (and torque) is toward the metal side, due to the low emissivity and a high reflectivity of the metal.
- One has to go to third order to see forces and torques on bodies made of homogeneous material. This will be discussed in future work.

Acknowledgments

This work was supported in part by a grant from the US National Science Foundation, grant number 2008417. We thank Steve Fulling, Xin Guo, and Prachi Parashar for collaborative assistance. This paper reflects solely the authors' personal opinions and does not represent the opinions of the authors' employers, present and past, in any way.

References

1. X. Guo, K. A. Milton, G. Kennedy, W. P. McNulty, N. Pourtolami, and Y. Li, *Phys. Rev. D* **104**, 11606 (2021).
2. X. Guo, K. A. Milton, G. Kennedy, W. P. McNulty, N. Pourtolami, and Y. Li, *Phys. Rev. D* **106**, 016008 (2022).
3. X. Guo, K. A. Milton, G. Kennedy, N. Pourtolami, *Phys. Rev. A* **107**, 062812 (2023)
4. K. A. Milton, X. Guo, G. Kennedy, N. Pourtolami, and D. M. DelCol, *Phys. Rev. A* **108**, 022809 (2023).
5. G. Kennedy, *Eur. Phys. J. Spec. Top.* **232**, 3197 (2023).
6. K. A. Milton, N. Pourtolami, and G. Kennedy, *Phys. Rev. A* **110**, 042814 (2024).
7. K. A. Milton, N. Pourtolami, and G. Kennedy, in preparation.
8. B. Strekha, S. Molesky, P. Chao, M. Krüger, and A. Rodriguez, *Phys. Rev. A* **106**, 042222 (2022).
9. K. Milton and J. Schwinger, *Classical Electrodynamics*, 2nd edn. (CRC Press, Boca Raton, 2024).
10. M. T. H. Reid, O. D. Miller, A. G. Polimeridis, A. W. Rodriguez, E. M. Tomlinson, and S. G. Johnson, arXiv:1708.01985, unpublished.
11. J. R. Deop-Ruano, F. J. García de Abajo, and A. Manjavacas, *Nanophotonics* (2024) <https://dpo.org/10.1511/nanoph-2024-0121>.